

# Quantum Measurement-Integrated Simulation of the Nonlinear Schrödinger Equation

Ann Author\* and Second Author†

*Authors' institution and/or address*

(Dated: December 4, 2023)

The Nonlinear Schrödinger Equation (NLSE) describes the time evolution of various physical systems, such as a Bose-Einstein condensate. This work proposes a quantum algorithm which simulates a system that evolves under the NLSE given a potential function. Unlike conventional Hamiltonian simulations, our approach involves a novel step where the nonlinear term of the Hamiltonian is derived by measuring the current quantum circuit's probability distribution at each timestep. Using Qiskit, a Python library for quantum computing, we conducted simulations to assess the accuracy of our method compared to the numerical solution. Key simulation parameters, including timestep size, total simulation duration, and the number of measurements at each timestep, were varied to understand their influence on simulation accuracy. Our findings reveal a specific scaling relationship of the simulation error with these parameters, which we have also substantiated through theoretical derivations. This research not only introduces a new quantum algorithm for NLSE system simulations but also provides critical insights into the dependencies of simulation accuracy on various operational parameters.

## I. INTRODUCTION

In recent years, quantum computing has become an emerging field with the potential to revolutionize our understanding and simulation of quantum systems. The intricacies of quantum mechanics, especially in nonlinear regimes, pose significant challenges that classical computational methods struggle to address efficiently. This is particularly evident in the context of the Nonlinear Schrödinger Equation (NLSE), a fundamental equation in quantum mechanics that describes the time evolution of complex, nonlinear systems, such as Bose-Einstein condensates and nonlinear optical fibers [1]. Traditional computational methods, while effective in linear domains, often fall short in capturing the full spectrum of dynamics governed by the NLSE.

In recent advancements in quantum simulation, considerable progress has been made in developing methods for simulating complex quantum systems. Quantum algorithms have demonstrated potential efficiencies over classical mean-field methods, particularly in simulating exact electron dynamics [2]. Notably, generalized NLSEs have been explored within the framework of Bohmian mechanics to describe dissipative and stochastic dynamics in quantum systems [3]. Furthermore, research into the Bose-Einstein condensation of photonic Bose gases and quantum models for electromagnetic wave propagation in highly nonlinear optical fibers has underscored the complexity and practical relevance of NLSE simulations [4, 5]. These studies collectively highlight the evolving landscape of quantum simulation.

However, an inherent challenge in simulating the NLSE using classical computational approaches lies in its nonlinearity; the equation includes terms where the potential is a function of the wavefunction itself. This charac-

teristic fundamentally diverges from linear quantum mechanics, where the time evolution is governed by a time-dependent Hamiltonian independent of the wavefunction. Consequently, traditional simulations that effectively handle linear, time-independent or time-dependent Hamiltonians encounter significant hurdles when applied to the NLSE. The feedback loop created by the wavefunction influencing the potential, which in turn affects the wavefunction's evolution, presents a complex computational problem. This limitation of conventional methods underscores the necessity of exploring new paradigms in quantum simulation, particularly the application of quantum computing techniques that can inherently accommodate such nonlinear dynamics.

Building on the foundation of recent advancements in quantum simulation, our research draws inspiration from Meyer and Wong's work on nonlinear quantum search [6]. Their exploration into the integration of nonlinear dynamics into quantum computing, specifically through the application of the Gross-Pitaevskii equation in quantum search algorithms, mirrors our venture into applying nonlinear principles in quantum simulations. While Meyer and Wong's work is oriented towards algorithmic optimization, our study pivots this concept towards the simulation of physical systems, particularly those governed by the NLSE, thereby broadening the scope of nonlinear dynamics in quantum computing.

In our research, we developed an innovative quantum algorithm to simulate the NLSE, with a focus on understanding how various simulation parameters affect accuracy. This involved a detailed analysis of the impact of timestep size ( $\Delta t$ ), simulation duration ( $T$ ), and the number of measurements per timestep ( $M$ ) on the simulation's precision. Our objective was to systematically explore and document the relationship between these parameters and the accuracy of the simulation, offering insights into the balance between computational resources and simulation accuracy.

---

\* Also at Physics Department, XYZ University.

† Second.Author@institution.edu

## II. BACKGROUND

The 1-dimensional NLSE with a potential  $V(x)$  is the partial differential equation

$$i \frac{\partial}{\partial t} \psi(t, x) = \left( -\frac{1}{2} \frac{\partial^2}{\partial x^2} + V(x) - g|\psi(t, x)|^2 \right) \psi(t, x) \quad (1)$$

where  $g$  is a positive constant. In our approach to quantum simulation, we addressed the challenge of representing the NLSE within the finite framework of a quantum computer by discretizing its spatial domain. Given that quantum computers are limited by a finite number of qubits, we must transform the continuous space of the NLSE into a discrete lattice that represents the continuous physical system by a discrete set of points  $\{x_0, x_1, \dots\}$ . We then construct an underlying graph  $G$  to represent the discretized space, where the vertices of  $G$  correspond to  $\{x_0, x_1, \dots\}$ , and the edges of  $G$  represent the interaction terms that link adjacent vertices, effectively capturing the local connectivity of the system.

Consider the transformation of the wavefunction  $\psi$  under discretization. In the continuous domain,  $\psi(t, x)$  is a complex-valued function representing the quantum state of the system at every point in space and time. When we transition to the discrete lattice,  $\psi$  is no longer a function of the continuous variable  $x$ , but instead becomes a vector whose elements correspond to the value of the wavefunction at the discrete nodes  $\{x_0, x_1, \dots\}$ , denoted as  $(\psi(t, x_0), \psi(t, x_1), \dots) = |\psi(t)\rangle$ .

Thus, if we discretize (1), the NLSE becomes a system of ordinary differential equations

$$i \frac{d|\psi(t)\rangle}{dt} = (-\gamma L + V - gK(t)) |\psi(t)\rangle \equiv H(t) |\psi(t)\rangle \quad (2)$$

where  $V$  is the diagonal matrix

$$V = \begin{pmatrix} V(x_0) & & & \\ & V(x_1) & & \\ & & V(x_2) & \\ & & & \ddots \end{pmatrix},$$

$K(t)$  is the diagonal matrix

$$K(t) = \begin{pmatrix} |\psi(t, x_0)|^2 & & & \\ & |\psi(t, x_1)|^2 & & \\ & & |\psi(t, x_2)|^2 & \\ & & & \ddots \end{pmatrix},$$

$\gamma = \frac{1}{2\Delta x^2}$ , and  $L$  is the Laplacian with the form  $L = A - D$ , where  $A$  is the adjacency matrix of  $G$  ( $A_{xy} = 1$  if  $\{x, y\}$  is an edge in  $G$ ,  $A_{xy} = 0$  otherwise) and  $D$  is the diagonal matrix with  $D_{xx}$  being the degree of vertex  $x$ .

## III. METHODOLOGY

### A. Setup

In this study, we have chosen specific initial conditions when we began the simulations. They were selected as follows:

- $G$  is the complete graph with 8 vertices. Thus the number of qubits required for the simulations is  $n = \log_2 8 = 3$  **why did we choose this?**

•

$$V(x) = \begin{cases} 1 & \text{if } x = x_0 \\ 0 & \text{otherwise} \end{cases}$$

- $|\psi(0)\rangle = \frac{1}{\sqrt{2^n}} \sum_{j=0}^{2^n-1} |j\rangle$ , the equal superposition of all basis states **why did we choose this?**

This setup provides a controlled environment for the simulations. The effects of changing all the other variables will be discussed in later sections.

### B. Algorithm Description

The core of our research involves a quantum simulation algorithm, specifically designed to simulate the NLSE for some time period  $T$  with timestep size  $\Delta t$  and number of measurements  $M$ . The algorithm follows these steps:

- Initialize the qubits to  $|\psi(0)\rangle$
- For  $t = 0, \Delta t, 2\Delta t, \dots, T - \Delta t$ :
  - Construct the Hamiltonian  $H(t)$  given by (2)
  - Apply the time evolution operator to get  $|\psi(t + \Delta t)\rangle = \exp(-iH(t)\Delta t)|\psi(t)\rangle$
  - Perform  $M$  measurements on  $|\psi(t + \Delta t)\rangle$  to get the probabilities of each basis  $|\psi(t + \Delta t, x_j)|^2, 0 \leq j < 2^n$

In developing a quantum algorithm for the NLSE, we venture into relatively unexplored territory, as no existing quantum algorithm is specifically tailored for this purpose. The NLSE's unitary yet nonlinear nature poses unique challenges, distinct from those addressed by traditional Hamiltonian simulation algorithms.

Our approach dynamically computes the Hamiltonian  $H(t)$  at each timestep based on the evolving state vector  $|\psi(t)\rangle$  by measuring the current quantum circuit. This method is crucial for accurately capturing the nonlinear dynamics of the NLSE, which traditional algorithms, designed for linear and time-independent Hamiltonians, might fail to fully represent.

The key hypothesis driving our algorithm is that a dynamically updated Hamiltonian, reflecting the state-dependent nature of the NLSE, can effectively simulate its complex evolution. Success in this endeavor could significantly broaden the capabilities of quantum simulations, allowing for more accurate modeling of nonlinear quantum systems.

### C. Parameter Variation

To explore the relationship between various parameters of the simulation and the error produced, we systematically varied the following parameters:

- $\Delta t$ : We conducted the simulation for  $0.01 \leq \Delta t \leq 0.09$ . Smaller time steps were hypothesized to produce more accurate results but at the cost of increased computational time.
- $M$ : We conducted the simulation for  $M \in \{2048, 4096, \infty\}$ . For  $M = \infty$ , the probabilities are directly obtained by squaring the statevector  $|\psi(t + \Delta t)\rangle$ . Larger number of measurements were hypothesized to produce more accurate results but at the cost of increased computational time.
- $t$ : We also observed how the accuracy is affected as the duration of the simulation increased, for  $0 \leq t \leq T = 50$ .

### D. Error Analysis

Due to the inherent complexity of the NLSE, obtaining an analytical solution tend to be extremely challenging, if not infeasible. Therefore, we adopted a comparative approach to quantify the error in our simulations. To assess the accuracy of our simulation, we compared the results obtained from our algorithm to the numerical solution obtained via the Runge-Kutta 45 (RK45) method.

For each set of parameters  $(\Delta t, M)$ , from our algorithm we obtain  $\psi_{\Delta t, M}(t, x_j)$  for  $0 \leq j < 2^n, t \leq T$ . However, given our initial condition that  $G$  is a complete graph and only vertex  $x_0$  has a potential, we know that at a fixed  $t$ ,  $|\psi_{\Delta t, M}(t, x_j)|^2$  is the same for  $1 \leq j < 2^n$  and

$$|\psi_{\Delta t, M}(t, x_j)|^2 = 1 - \frac{1}{2^n - 1} |\psi_{\Delta t, M}(t, x_0)|^2$$

If we are only interested in the probability distribution of our simulation, then it is sufficient to compare  $|\psi_{\Delta t, M}(t, x_0)|^2$  to the numerical solution. In order to do so, we compute the expected error of

$$|\psi_{\Delta t, M}(t, x_0)|^2 \equiv P_{\Delta t, M}(t)$$

Define the numerical solution of the probability of  $x_0$  to be  $\hat{P}(t)$ , then the mean absolute error is

$$\text{MAE}_{\Delta t, M}(t) = \frac{1}{N} \sum_{k=1}^N |P_{\Delta t, M}^k(t) - \hat{P}(t)| \quad (3)$$

where we ran the simulation for  $N = 500$  times and  $P_{\Delta t, M}^k(t)$  denotes the probability on the  $k$ -th simulation. Multiple runs are essential to account for the randomness introduced by measurements. They provide a way to average out random fluctuations and reveal the underlying deterministic trends of the system.

## IV. RESULTS

Our simulation results showed the intricate dynamics of the NLSE under various conditions. By systematically altering key simulation parameters, we have gained insights into their distinct roles and the interplay between them. The following subsections detail the effects of these variables.

### A. Simulation Duration $t$

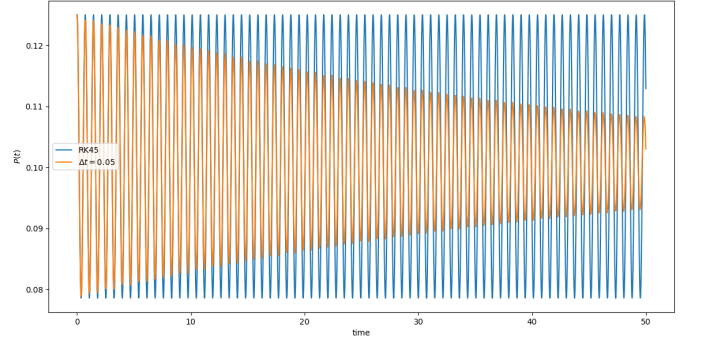


FIG. 1. adfasfd

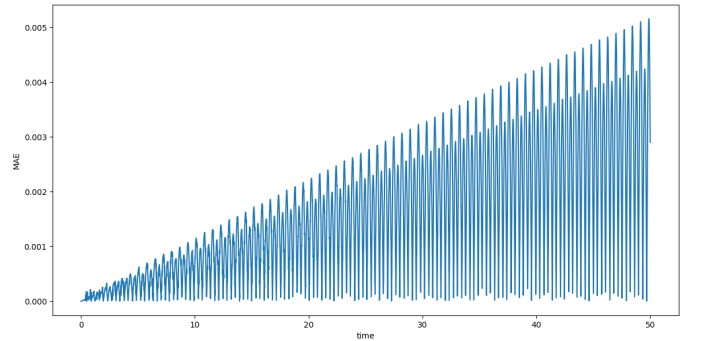


FIG. 2. adfasfd

Fig. 1 shows the comparison of  $P_{0.01, 8192}(t)$  and  $\hat{P}(t)$  for  $0 \leq t \leq 50$ . Both curves exhibit oscillatory patterns with a constant frequency and their phases are almost in sync; however,  $\hat{P}(t)$  maintains a consistent amplitude, while the amplitude of  $P_{0.01, 8192}(t)$  decreases over time. Later we will show that this pattern generally holds true for other values of  $\Delta t$  and large enough  $M$ .

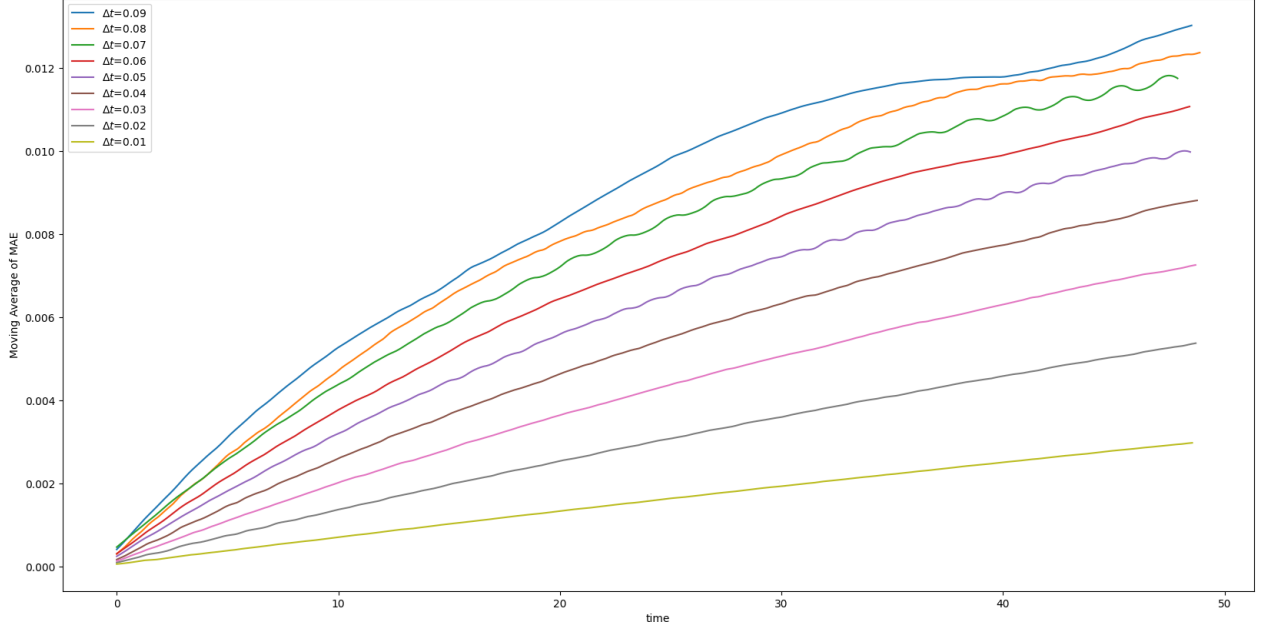


FIG. 3. adfasfd

Fig. 2 shows how the error  $\text{MAE}_{0.01,8192}(t)$  grows over time. However, to better understand the underlying trend of the error without the oscillatory behavior, we applied a moving average with a window size equal to the oscillation period of the error. This technique smooths out the fluctuations, allowing us to discern a non-oscillatory pattern in the error's behavior over time. The moving average effectively filters out the high-frequency components, revealing any long-term trends in the simulation's accuracy.

Fig. 3 shows the moving average of the error over time for various  $\Delta t$ . After applying a moving average to smooth out the oscillations in the error, we have fitted the resulting data to an exponential model of the form  $a - be^{-\lambda t}$ , where  $b$  and  $\lambda$  are positive and  $a$  represents the asymptotic value that the error approaches as  $t \rightarrow \infty$ , as shown in Fig. 5 for some values of  $\Delta t$ . The goodness of fit for this model is exceptionally high across all values of  $\Delta t$  as indicated by  $R^2$  values of around 0.9999. Moreover, the Mean Squared Errors (MSEs) for these fits are in the order of  $10^{-11}$  to  $10^{-9}$ , suggesting that the exponential model closely captures the underlying trend of the error's growth.

Thus, combining the oscillatory and non-oscillatory components of the error, a plausible representation of the error as a function of time has the form

$$(a - be^{-\lambda t}) \cos(\omega t), \quad (4)$$

where  $\omega$  is the oscillation frequency of the  $\hat{P}(t)$ . The exponential term  $a - be^{-\lambda t}$  indicates a compounding effect where errors grow larger with each successive timestep. Meanwhile, the cosine factor  $\cos(\omega t)$  reflects a consistent oscillation in the error, potentially mirroring periodic dy-

namics within the simulated quantum system. A more detailed analysis will be provided in later sections.

## B. Timestep Size $\Delta t$

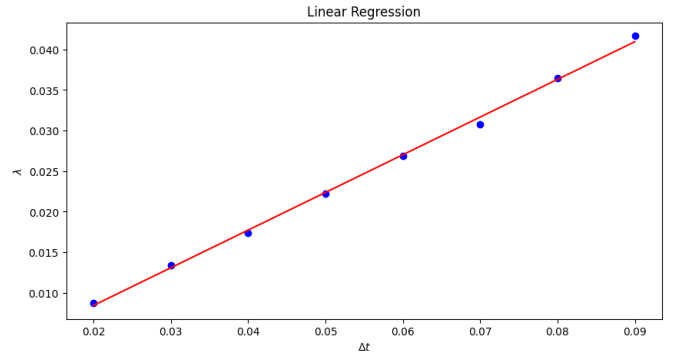


FIG. 4. adfasfd

Next, we discuss the relationship between the timestep size  $\Delta t$  and the simulation error. As mentioned in the previous section, we have quantitatively analyzed the error over time by fitting the error for different  $\Delta t$  to exponential models of the form  $a - be^{-\lambda t}$ . Remarkably, we observed that while the parameters  $a$  and  $b$  remain relatively constant across different  $\Delta t$ , the parameter  $\lambda$ , which represents the rate of exponential decay of the error, exhibits a linear relationship with  $\Delta t$ .

The consistency in the values of  $a$  and  $c$  suggests that the initial error scale and the baseline offset are not significantly influenced by the choice of time step size. How-

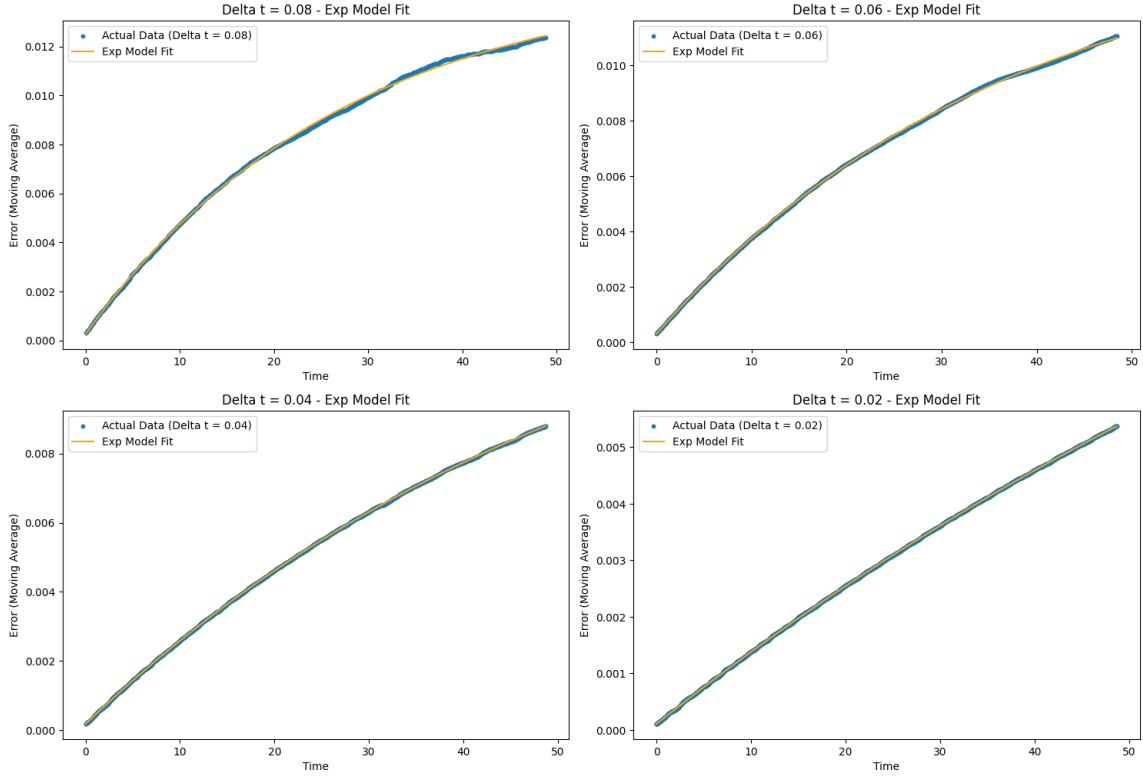


FIG. 5. adfasfd

ever, the parameter  $\lambda$ , crucially, indicates that the rate at which the error increases over time is directly proportional to  $\Delta t$ . As shown in Fig. 4, the magnitude of  $\lambda$  increases linearly with  $\Delta t$ . This linear dependence underscores a key finding: as we increase the time step size, we proportionally accelerate the error's growth rate within the simulation. Conversely, reducing  $\Delta t$  slows down this rate, enhancing the simulation's long-term stability and accuracy.

Thus, if we replace  $\lambda$  with a linear equation  $\lambda = k\Delta t + d$  in Eq. (4), we get a function in the form

$$(a - be^{-(k\Delta t + d)t}) \cos(\omega t) \quad (5)$$

that describes the error in terms of  $t$  and  $\Delta t$

### C. Number of Measurements $M$

As shown in Fig. 6, an increase in  $M$  correlates with a decrease in the error over time, indicating an inverse relationship between the number of measurements and simulation error as expected. The data for  $M = 32$  and  $M = 64$  demonstrate a steeper error trajectory compared to higher values of  $M$ , while the data for  $M = 128$  shows a slightly higher error compared to higher values of  $M$ . For  $M$  values of 1024 and higher, the error is almost indistinguishable from the error at  $M = \infty$ , suggesting a saturation point beyond which additional measurements do not yield a noticeable improvement in simulation accuracy.

Thus, while higher number of measurements contributes to a higher accuracy in simulating the NLSE, our results indicate that given our initial conditions, an  $M$  value of 1024 may be sufficient for capturing the dynamics of the system to a degree comparable with continuous measurement. This finding is instrumental for the optimization of quantum simulations, highlighting a specific range for  $M$  that provides a balance between simulation fidelity and computational resource allocation.

- 
- [1] B. Malomed, Nonlinear schrödinger equations (2005).
  - [2] R. Babbush, W. J. Huggins, D. W. Berry, S. F. Ung,

- A. Zhao, D. R. Reichman, H. Neven, A. D. Baczewski, and J. Lee, Quantum simulation of exact electron dynam-

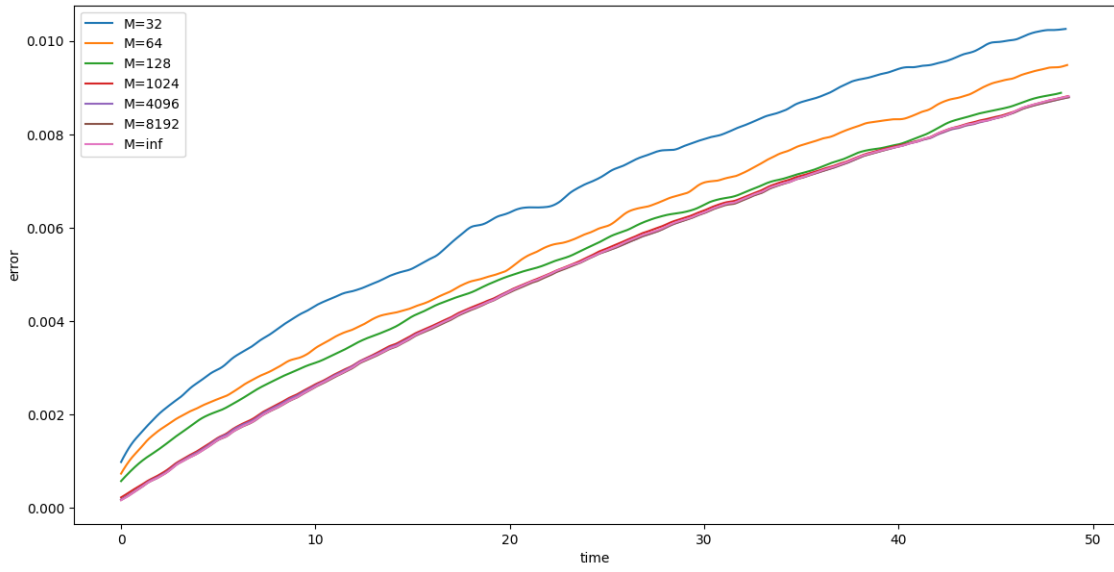


FIG. 6. adfasfd

ics can be more efficient than classical mean-field methods, Nat. Commun. **14** (2023).

- [3] S. Mousavi and S. Miret-Artés, On non-linear schrödinger equations for open quantum systems, Eur. Phys. J. Plus **134**, 10.1140/epjp/i2019-12965-6 (2019).
- [4] M. Vretnar, C. Toebes, and J. Klaers, Modified bose-einstein condensation in an optical quantum gas, Nat.

Commun. **12** (2021).

- [5] A. Safaei Bezgabadi and M. Bolorizadeh, Quantum model for supercontinuum generation process, Sci. Rep. **12** (2022).
- [6] D. A. Meyer and T. G. Wong, Nonlinear quantum search using the gross-pitaevskii equation, New Journal of Physics **15**, 10.1088/1367-2630/15/6/063014 (2013).